processes

MDPI

Article

A Flexible Heat Exchanger Network Synthesis Method Adapted to Multi-Operation Conditions

Sibei Ji, Li Zhou *, Bozhou Dang, Xu Ji and Yagu Dang

School of Chemical Engineering, Sichuan University, Chengdu 610065, China; 2021223070019@stu.scu.edu.cn (S.J.); danielboatdang@outlook.com (B.D.); jxhhpb@163.com (X.J.); derkdang@scu.edu.cn (Y.D.)

* Correspondence: chezli@scu.edu.cn; Tel.: +86-152-2886-7167

Abstract: This paper presents a flexible HEN (heat exchanger network) synthesis methodology for designing a multiperiod HEN with streams involving phase changes. The methodology is based on an MINLP (mixed integer nonlinear programming) model, identification of critical points, and flexibility index analysis considering phase changes. A nominal multiperiod HEN topology is constructed in the first step. Then each process operating condition's critical points and flexibility index are calculated to verify the feasibility of the designed HEN under multiple operating conditions. To verify the validity of the method, the proposed methodology will be applied to a case study on an ammonia synthesis process heat transfer network design based on renewable energy. The results show that the method can obtain a flexible heat transfer network that is cost-effective and adaptable to multi-condition production for green ammonia synthesis.

Keywords: heat exchanger network; flexibility; multiperiod; stream phase changes

check for updates

Citation: Ji, S.; Zhou, L.; Dang, B.; Ji, X.; Dang, Y. A Flexible Heat Exchanger Network Synthesis Method Adapted to Multi-Operation Conditions. *Processes* **2023**, *11*, 2734. https://doi.org/10.3390/pr11092734

Academic Editor: Ireneusz Zbicinski

Received: 10 August 2023
Revised: 1 September 2023
Accepted: 6 September 2023
Published: 13 September 2023

1. Introduction

HENs (heat exchanger networks) are essential for the energy recovery of chemical production processes. HEN synthesis and optimization are important strategies for process energy efficiency enhancement. The development of techniques for systematic HEN design is progressing quickly, from sequential methods [1] to simultaneous synthesis methods, for example, the well-studied hierarchical superstructure-based methodology developed by Yee and Grossmann [2]. Mihaela and Paul [3] summarized the representative research advances in heat transfer network synthesis from 1975 to 2008. The research progress of the heat exchanger network synthesis methods is also described in the papers of Wang and Feng [4] in detail.

Industrial processes often experience changes from upstream raw material supply and/or downstream product market demand, leading to changes in process production load. Hence, one HEN will experience several different operation conditions when different production load is ongoing. In such cases, differences in stream properties (flow rates, temperature, component concentration, etc.) of different operation periods need to be considered to guarantee the accuracy and practicability of the resulting HEN.

Numerous multiperiod operation HEN synthesis methods have been developed in the past decades. Huang and Karimi [5] proposed a multiperiod superstructure that allows reflux and splitting. To develop a more systematic approach to the multiperiod HEN design problem, Isafiade et al. [6] modified the stage-wise superstructure (SWS) model by Yee and Grossmann [2] to deal with the synthesis of HEN with multiple operating periods. To further simplify the generation of HEN, Kang et al. [7] proposed a representative subperiod approach to synthesize multiperiod HEN, in which the longest duration subperiod is chosen as the representative subperiod for the HEN. This method was further improved by Isafiade et al. [8], where the worst run period was selected as the representative subperiod to cope with problems such as the variation of the subperiod. To completely use cheap

and environmentally friendly renewable energy, Isafiade et al. [9] proposed a multiperiod HEN synthesis method that allows the selection of different utility combinations based on different periods or seasons of operation. It is worth mentioning that most of the above methods are carried out in fixed operating conditions. But, very often, the operational condition of a system experiences disturbances. In order to produce a more practical HEN which can adapt to the disturbance of parameter fluctuations, the values of the uncertain parameters should be considered rather than set as a fixed value.

Marselle et al. [10] first introduced the concept of resilient designs as a solution to cope with the uncertainty of industrial design. The flexibility index, proposed by Swaney and Grossmann [11], is usually used to measure a system's adaptability to various operating conditions. It indicates the maximum deviation from the nominal point of the uncertain parameters which the HEN can meet without causing process difficulties.

Flexibility indexes are widely used in process integration, and more advanced methods have emerged. Konukman et al. [12] proposed a HEN synthesis method that synthesizes the optimal solution of HEN as the lower bound of utilities satisfying the flexibility index. In 2015, Pintarič and Kravanja [13] presented a novel computational approach to stepwise synthesis and design of flexible HEN with many uncertain parameters through methods such as critical point identification [14] and sensitivity analysis [15].

For multiperiod HEN synthesis, flexibility analysis and flexibility indexes were also introduced. Papalexandri and Pistikopoulos [16] developed a multiperiod MINLP model for the flexible synthesis of heat and mass exchange separation processes. Verheyen and Zhang [17] published a simultaneous MINLP model for the design of multiperiod HEN, proving that the model of Yee and Grossmann [2] can be used for multiperiod HEN designs by eliminating the average area assumption of Aaltola [18] and obtaining more satisfactory results. The paper by Kang et al. [19] in 2018 discussed a three-step method for the design of a flexible multiperiod HEN when uncertain parameter fluctuations occur at subperiods. First, a nominal multiperiod HEN is generated, then critical point identification and flexibility tests are applied to the HEN. The flexible improvement model is solved if the flexibility is not up to standard. The method is verified through a case study.

Although many proposed HEN generation methods are well-established, investigation is still needed for processes where streams experience phase changes. Since phase changes play a significant role in many thermal processes, methods that do not account for phase changes may derive biased heat transfer driving forces and underestimate heat transfer area. On account of phase changes, Jose et al. [20] presented an MINLP model that considers several flow units designed for heat transfer in industrial processes, such as the nonisothermal streams only with sensible heat, the isothermal streams only with latent heat, and the streams with both latent heat and sensible heat. The paper by William et al. [21] in 2014 summarized the issues that should be noted and avoided when considering phase changes. For example, because of the small differential temperature driving forces, the actual total heat transfer area should be much bigger than the heat transfer area calculated by the simple model without consideration of phase changes. Yeong et al. [22] proposed a graphical method for HEN targeting and network design involving phase changes.

However, HEN synthesis methods that simultaneously adapt parameter fluctuations and phase changes have not been thoroughly studied. To fill this gap, this paper proposes a flexible multiperiod HEN synthesis method that can be adapted to the phase change process while considering multiperiod HEN operation. Identifying the critical operation points and calculating the flexibility index are involved. The rest of the paper is structured as follows. First, the design problem concerning a flexible multiperiod HEN with phase changes is described. Next, a detailed solution is suggested, ensuring the flexibility and economic effectiveness of the HEN. Finally, conclusions are drawn after verifying the method using an ammonia synthesis case study.

2. Problem Statement

When different operating conditions are involved, fluctuations in stream parameters (such as flow rates, temperature, and vapor fraction) should be considered in network synthesis in order to obtain a more accurate and flexible HEN.

The flexible HEN integration problem considered in this work is described as in the following. There are i hot and j cold streams of a chemical process that need to be matched for heat recovery. The relevant parameters are as follows:

Nominal operating conditions in several operation periods. For example, the initial temperature and the targeted temperature, the heat capacity flow rates, the initial vapor fraction of the stream, and the concentration of the involved materials in the streams in each operation period.

Utility-related parameters. For example, the initial temperature of the cold and hot utility, as well as the corresponding unit price.

Variation ranges of the considered uncertain parameters. For example, the initial temperature, the heat capacity flow rates, as well as the initial vapor fraction of the streams.

It is required to generate a HEN design that is flexible enough to cope with the fluctuation of uncertain parameters during the involved operation conditions. To that end, the following information needs to be determined: (1) the matches of the cold and hot streams; (2) the required heat exchange area of each heat recovery match; (3) the consumption of hot and cold utility. Additionally, phase changes that may occur during operation need to be identified in order to obtain a more practical HEN.

3. The Proposed Flexible HEN Synthesis Method

This section describes the proposed method in detail. The flow chart of the method is shown in Figure 1.

In this method, the original combination of uncertainty parameter values for each subperiod is set to the nominal point. θ^N are the nominal values of uncertain parameters. In order to limit uncertain parameters θ, $\Delta\theta^+$, and $\Delta\theta^-$ are introduced as the expected variation in a positive or negative direction. After critical point identification, θ_s represents the value of uncertain parameters in each critical point, and$\Delta\theta_s$ represents the expected variation of uncertain parameters corresponding to critical point s.

3.1. Nominal Multiperiod HEN Topology Generation

The topology of the nominal multiperiod HEN, including the number of heat exchangers, the matching of hot and cold streams, the heat exchange area assignment, etc., is obtained by solving Model A. Since Model A is a single-period problem, the representative subperiod method [7] will determine the subperiod used to solve Model A nominally with θ^N. By determining the structure of the nominal HEN, the heat transfer areas in the rest of the non-representative subperiods are optimized by solving Model A with a fixed nominal structure.

The model is extended from the stage-wise superstructure-based method proposed by Yee and Grossmann [2] in Figure 2, by including the calculation for parameters related to phase changes in streams, for example, the identification of phase changes for the streams, the calculation of material content in a stream when the phase changes occurs, and the consideration of the latent heat of vaporization for the energy balance in heat recovery matching when vaporization is involved. In a stage-wise superstructure, note that (1) heaters can only occur before stage 1 and coolers can only occur after stage k; (2) for each stream, only one heat transfer match is allowed to exist within a stage; (3) in each stage, hot streams exchange heat with cold streams, and finally reach the targeted temperature at the end of the HEN; (4) in this model, stream splitting is not allowed.

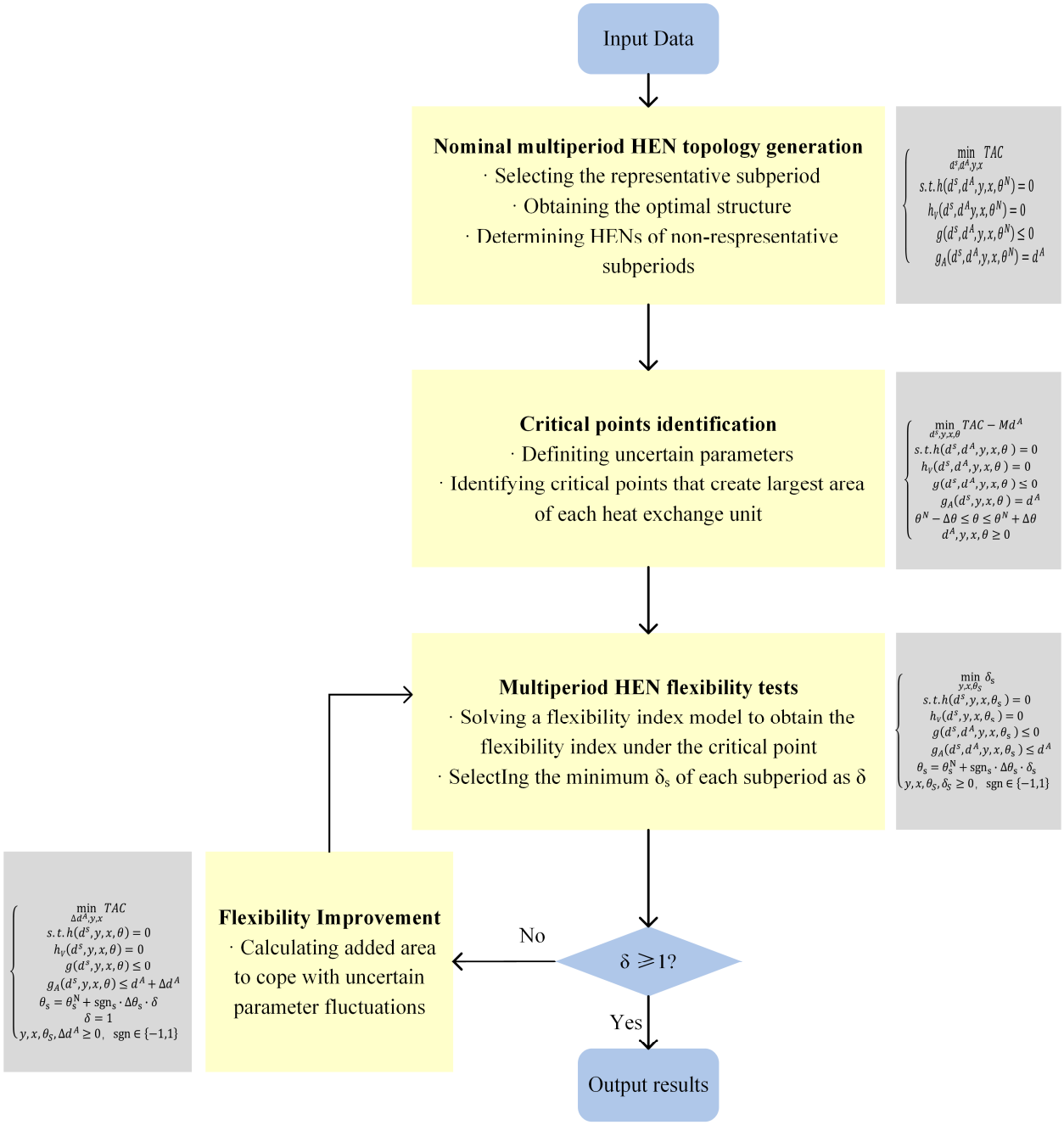

Figure 1. A flexible heat exchanger network synthesis method adapted to a multi-condition ammonia process.

The objective function Model A:

$$Obj\ \min_{x,y} TAC = c_f\left(\sum_{i,j,k} z_{i,j,k} + \sum_j zhu_j + \sum_i zcu_i\right) + c_A\left(\sum_{i,j,k}\left(A_{i,j,k}\right)^{\beta} + \sum_j\left(Ahu_j\right)^{\beta} + \sum_i\left(Acu_i\right)^{\beta}\right) + c_{hu}\sum_j\left(qhu_j\right) + c_{cu}\sum_i\left(qcu_i\right)$$

subject to equality constraints (A1)–(A6); inequality constraints (A7)–(A12); equality area constraints (A13); as well as the phase change constraints, which will be discussed in the

following. Detailed constraint equations can be found in Appendix A. In this objective function, TAC is the total annual cost of subperiods of the HEN, which is set as the objective function. c_f, c_A, c_{hu}, and c_{cu} represent the cost coefficient of the heat exchanger, heat transfer area, cooling utility, and heating utility, respectively; $z_{i,j,k}$, zhu_j, and zcu_i are the binary variables representing the existence of each heat exchanger of hot stream i and cold stream j match at stage k, cooler for hot stream i, and heater for cold stream j, respectively; $A_{i,j,k}$, Ahu_j, and Acu_i represent the corresponding heat transfer area of each heat exchange unit; $q_{i,j,k}$, qhu_j, and qcu_i represent the corresponding heat load of each heat exchange unit. β is the cost exponent of the heat transfer area.

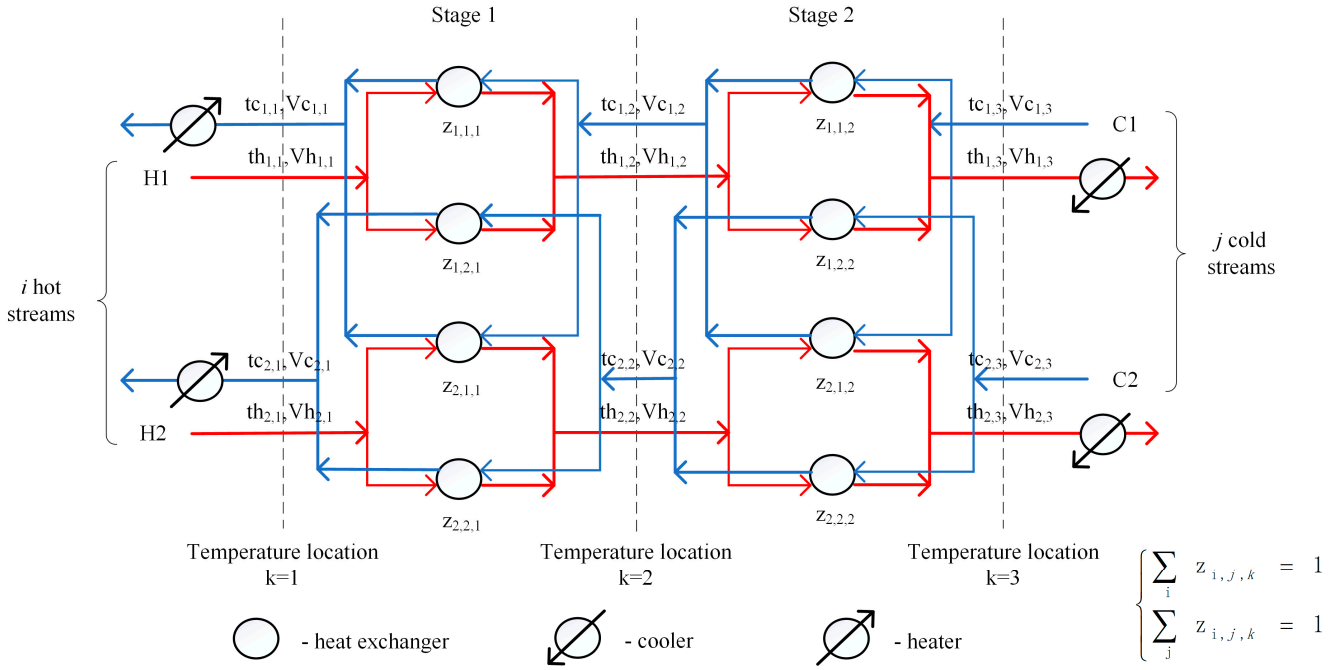

Figure 2. Heat exchanger network stage-wise superstructure.

The Antoine formula, a mathematical expression of the relation between the vapor pressure and the temperature, is adopted to determine the saturated vapor pressure of the process streams:

$$\log Ph^*_{x,i,k} = A - \frac{B}{th_{i,k} + C} \tag{1}$$

$$\log Pc^*_{x,j,k} = A - \frac{B}{tc_{j,k} + C} \tag{2}$$

where $Ph^*_{x,i,k}$, $Pc^*_{x,j,k}$ are the saturation vapor pressure of component x, which is of interest. In this work, it is the produced ammonia. $th_{i,k}$ and $tc_{j,k}$ are the temperature of the hot and cold streams in stage k. A, B, and C are the Antoine coefficients.

The calculated saturation vapor pressure is then used to determine whether phase changes occur. As shown in Equations (3) and (4), when the calculated saturation vapor pressure $Ph^*_{x,i,k}$ is smaller than $Ph_{x,i}$, the partial pressure of component x is in stream i, and the initial vapor fraction Vhin is not equal to 0, the sign function $\mathrm{sgn}\left(Ph_{x,i} - Ph^*_{x,i,k}\right)$ takes value 1, then $zh_{i,k}$ equals 1, indicating that the hot stream i will experience a phase change in stage k. If the calculated saturation vapor pressure $Ph^*_{x,i,k}$ is larger than the partial pressure of component x in stream i, or the initial vapor fraction Vhin is equal to 0, the

sign function $\mathrm{sgn}\left(Ph_{x,i} - Ph^{*}_{x,i,k}\right)$ takes value 0, then $zh_{i,k}$ equals 0, indicating that phase change will not occur. The same rule applies to the cold stream.

$$zh_{i,k} - \frac{1+\mathrm{sgn}\left(Ph_{x,i}-Ph^{*}_{x,i,k}\right)}{2} = 0 \tag{3}$$

$$zc_{j,k} - \frac{1+\mathrm{sgn}\left(Pc^{*}_{x,j,k} - Pc_{x,j}\right)}{2} = 0 \tag{4}$$

The molar content of the substance of interest in the gas phase, y^{*}_{x}, is calculated using the Larson–Black empirical formula given in Equation (5) [23]:

$$\log y^{*}_{x} = \mathcal{A} + \frac{\mathcal{B}}{\sqrt{P}} - \frac{\mathcal{C}}{th_{i,k}} + \alpha \tag{5}$$

where $\mathcal{A}$, $\mathcal{B}$, and $\mathcal{C}$ denote the coefficients that take a specific value for a certain substance. P is the total pressure of the stream. α is the modified coefficient. In this work, the substance considered is ammonia, for which $\mathcal{A}$, $\mathcal{B}$, and $\mathcal{C}$ take values of 4.1856, 60.2724, and 1099.5, respectively.

In this work, the heat of vaporization of components for hot streams and cold streams, $Rh_{i,k}$, $Rc_{j,k}$, is calculated by fitting Equations (6) and (7):

$$Rh_{i,k} = \mathrm{a}\left(th_{i,k+1} - 273.15\right)^{2} + \mathrm{b}\left(th_{i,k+1} - 273.15\right) + \mathrm{c} \tag{6}$$

$$Rc_{j,k} = \mathrm{a}\left(tc_{j,k} - 273.15\right)^{2} + \mathrm{b}\left(tc_{j,k} - 273.15\right) + \mathrm{c} \tag{7}$$

which is used to calculate the heat load of streams with phase changes.

Then the vapor fraction $Vh_{i,k}$ of each stage of each hot stream is calculated by the following constraints (8):

$$Vh_{i,k} - zh_{i,k-1}\left(\frac{1 - X_{x,i}}{1 - y^{*}_{NH_3,\,i,\,k}} + \alpha\right) + (1 - zh_{i,k-1})Vh_{i,k-1} = 0 \tag{8}$$

where $X_{x,i}$ is the component content of x. $Vc_{j,k}$ of each stage of each cold stream is determined by the conservation of energy.

The final nominal multiperiod HEN structure is determined using the maximum area principles, which define the maximum area of a heat exchanger in each subperiod as the final assigned area.

3.2. Critical Point Identification

The scenario is a combination of the values of θ in the case. There are infinite combinations since the uncertain parameters are set as continuous variables restricted to a range. It is unrealistic to consider all combinations simultaneously, so reducing the number of scenarios is necessary. In this step, therefore, a single-scenario NLP Model B is introduced to control the number of scenarios to the number of heat exchange units. The model is repeated for each heat exchange unit, and the result of each optimization will be a combination of values of uncertain parameters representing the heat exchange unit's critical point.

An approximate one-level formulation [14] is chosen to save time and cost, as well as to avoid the enumeration of multiple scenarios. The objective function Model B is as follows:

$$Obj \min_{x,y} TAC = c_f \left(\sum_{i,j,k} z_{i,j,k} + \sum_j zhu_j + \sum_i zcu_i \right) + c_A \left(\sum_{i,j,k} \left(A_{i,j,k} \right)^\beta + \sum_j \left(Ahu_j \right)^\beta + \sum_i \left(Acu_i \right)^\beta \right) + c_{hu} \sum_j \left(qhu_j \right) + c_{cu} \sum_i \left(qcu_i \right) - MdA$$

subject to equality constraints (A1)–(A6); phase change constraints (1)–(8); inequality constraints (A7)–(A12); equality area constraints (A13); inequality uncertain parameter range constraints (9) and (10). In this objective function, d^A represents the heat transfer area of each exchanger unit, which includes heat exchanger $A_{i,j,k}$, heater Ahu_j, and cooler Acu_i. M is a large number, which is added to compromise the minimization of the TAC and maximization of the heat transfer areas.

The equations in Model B are the same as in Model A, except that the uncertain parameters are involved in the solution as variables, which is constrained by (9) and (10).

$$\theta^N - \Delta\theta^- \leq \theta \tag{9}$$

$$\theta \leq \theta^N + \Delta\theta^+ \tag{10}$$

3.3. Multiperiod HEN Flexibility Tests

After obtaining critical points, the superiority and adaptability of the design should be assessed. According to the results of the scenario selection in Model B, θ_s are chosen as the data for this step to calculate the flexibility index. Model C is also a single-scenario NLP problem, which is based on the model of Swaney and Grossmann [11] and is performed for each subperiod.

The objective function Model C is as follows:

$$Obj \max_{y,x,\theta_s} \delta_s$$

subject to equality constraints (A2)–(A6); phase change constraints (1)–(8); inequality constraints (A7)–(A10); inequality area Equations (11)–(13); equality uncertain parameter constraints (14). Model C contains only part of the equations for Model A and Model B.

Equality area constraints (A13) are replaced by inequality area constraints (11)–(13) to obtain the values of uncertain parameters, and Equation (14) is added to calculate the flexibility index:

$$A_{i,j,k} \geq \left(\frac{1}{u} + \frac{1}{u}\right) \frac{q_{i,j,k}}{\left(dt_{i,j,k} dt_{i,j,k+1} \left(dt_{i,j,k} + dt_{i,j,k+1}\right)/2\right)^{\frac{1}{3}}} \tag{11}$$

$$Ahu_j \geq \left(\frac{1}{u} + \frac{1}{u}\right) \frac{qhu_j}{\left(dthu_j \left(thu_{in} - tc_{out,j}\right) \left(dthu_j + thu_{in} - tc_{out,j}\right)/2\right)^{\frac{1}{3}}} \tag{12}$$

$$Acu_i \geq \left(\frac{1}{u} + \frac{1}{u}\right) \frac{qcu_i}{\left(dtcu_i \left(th_{out,i} - tcu_{in}\right) \left(dtcu_i + th_{out,i} - tcu_{in}\right)/2\right)^{\frac{1}{3}}} \tag{13}$$

$$\theta_s = \theta_s^N + \mathrm{sgn}_s \cdot \Delta\theta_s \cdot \delta_s \tag{14}$$

where sgn_n represents the direction of deviation from the nominal point towards the critical point; u represents heat transfer coefficients; $dt_{i,j,k}$, $dtcu_i$, $dthu_j$ represent the temperature differences of heat exchange units;thu_{in}, tcu_{in} are the initial temperature of hot utility and cold utility; δ_s represents the flexibility index of each critical point, which measures the size of the feasible operating region in uncertain parameters and constraint parameters within

which possible operation is guaranteed. If the value of the flexibility index of the HEN is equal to or greater than 1, the design of the HEN is feasible within an uncertain parameter range. The smaller the value ofδ_s, the smaller the degree of deviation.

After operating Model C, the flexibility index of each subperiod is defined as the minimum of all critical points by Model D.

The objective function Model D is as follows:

$$Obj\ \delta = \min_{s \in S} \delta_s$$

The flexibility index δ of the whole multiperiod HEN is finally determined as the minimum value of the flexibility indexes of the three subperiods.

3.4. Flexibility Improvement

In cases where the flexibility index is less than 1, a flexibility improvement of the nominal HEN is needed, which is carried out by increasing the heat transfer areas of the corresponding heat transfer units. This operation allows for a bigger heat transfer load and a smaller heat transfer temperature difference. Based on the obtained heat transfer structure, the heat transfer area, and the identified critical points, the solution is solved using the following model with the flexibility index set to 1.

The objective function Model E is as follows:

$$\begin{gathered} Obj \min_{x,y} TAC = c_f \left(\sum_{i,j,k} z_{i,j,k} + \sum_j zhu_j + \sum_i zcu_i \right) \\ +c_A \left(\begin{array}{c} \sum_{i,j,k} \left(A_{i,j,k} + \Delta A_{i,j,k} \right)^\beta + \sum_j \left(Ahu_j + \Delta Ahu_j \right)^\beta \\ +\sum_i \left(Acu_i + \Delta Acu_i \right)^\beta \end{array} \right) \\ +c_{hu} \sum_j \left(qhu_j \right) + c_{cu} \sum_i \left(qcu_i \right) \end{gathered}$$

subject to equality constraints (A1)–(A6); phase change constraints (1)–(8); inequality constraints (A7)–(A12); equality uncertain parameter constraints (14); inequality area constraints (15)–(17).

Model E contains most of the equations of Model A and Model B, where the equality area constraints (A13) are replaced by inequality area constraints (15)–(17) to solve for the heat transfer area that needs to be improved.

$$A_{i,j,k} + \Delta A_{i,j,k} \geq \left(\frac{1}{u} + \frac{1}{u} \right) \frac{q_{i,j,k}}{\left(dt_{i,j,k} dt_{i,j,k+1} \left(dt_{i,j,k} + dt_{i,j,k+1} \right) / 2 \right)^{\frac{1}{3}}} \tag{15}$$

$$Ahu_j + \Delta Ahu_j \geq \left(\frac{1}{u} + \frac{1}{u} \right) \frac{qhu_j}{\left(dthu_j \left(thu_{in} - tc_{out,j} \right) \left(dthu_j + thu_{in} - tc_{out,j} \right) / 2 \right)^{\frac{1}{3}}} \tag{16}$$

$$Acu_i + \Delta Acu_i \geq \left(\frac{1}{u} + \frac{1}{u} \right) \frac{qcu_i}{\left(dtcu_i (th_{out,i} - tcu_{in}) \left(dtcu_i + th_{out,i} - tcu_{in} \right) / 2 \right)^{\frac{1}{3}}} \tag{17}$$

where $\Delta A_{i,j,k}$, ΔAhu_j, and ΔAcu_i are the additional heat transfer areas of heat exchangers, coolers, and heaters. Nominal $A_{i,j,k}$, Ahu_j, and $Acu_i$are input as known data, while the flexibility index is set to 1, i.e., it should ensure that the improved HEN is guaranteed to adapt parameter fluctuations. The critical points of Model B are solved for each subperiod and each heat exchanger to obtain the corresponding $\Delta A_{i,j,k}$, ΔAhu_j, and ΔAcu_i. Finally, three kinds of areas are again confirmed using the maximum area principles, and $A_{i,j,k} + \Delta A_{i,j,k}$, $Ahu_j + \Delta Ahu_j$, and $Acu_i + \Delta Acu_i$ are the final assigned heat transfer area for each heat exchanger.

4. Case Study

To verify the feasibility of the proposed method, this paper uses it to design a multi-period flexible HEN for an actual case of ammonia synthesis process with phase changes. The mathematical programming software GAMS32.2 (General Algebraic Modeling System) was used, and the DICOPT solver was selected to be the global solver; NLP and MIP problems are solved by CONOPT4 and CPLEX, respectively.

4.1. Ammonia Synthesis Process

The emergence of synthetic ammonia has greatly influenced today's synthetic fertilizer industry. It is an important component of the traditional coal chemical industry. Most studies on ammonia systems have focused on energy saving and emission reduction in the synthesis section and on reducing economic inputs, such as Dong et al.'s [24] simulation and optimization of ammonia heat transfer networks in 2006 and Zhang et al.'s [25] analysis of heat transfer networks in ammonia systems based on the pinch point technique in 2018. The ammonia synthesis process is illustrated in Figure 3.

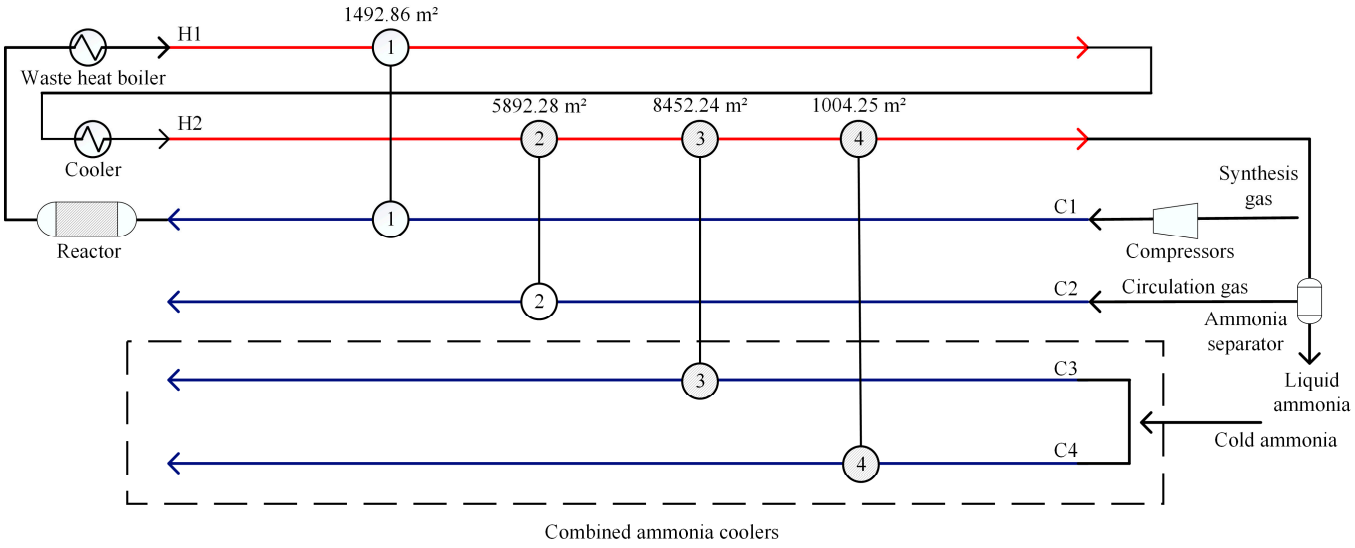

Figure 3. Structure of original ammonia synthesis process HEN.

The compressed synthesis gas is mixed with the circulating gas with 12% ammonia content and heated up into the ammonia synthesis tower, then the reactive gas with 19% ammonia content is cooled by water in the cooler and cold ammonia in the combined ammonia coolers to 273.15 K and separated from the system after completion. Then the circulation gas with 5% ammonia content is recycled.

4.2. Basic Data

According to an actual process, the ammonia synthesis has three subperiods representing 80%, 70%, and 60% operating load and 0.021, 0.024, and 0.0183 for the modified coefficients, respectively. The remaining operating data are defined in Table 1. H1 is the reactive gas after water heat boilers 123C; H2 is the reactive gas after water cooler 124C; C1 is the synthesis gas; C2 is the circulation gas; C3 and C4 are the cold ammonia. The material in the flow chart is divided and named into hot or cold streams according to different compositions, temperatures, flow rates, and specific heat capacities. The minimum approach temperature for all matches is set to 0.01 K. When there is a phase change in the streams, the process of phase change will release or absorb a large amount of heat, so that the heat transfer coefficient of the stream with a phase change is greater than that without a phase change. In order to simplify the calculation, the effect of phase change on the heat

transfer coefficient is not considered in this paper, and the overall heat transfer coefficient is set to 0.2. The remained coefficients are from the case of Kang et al.'s [19] paper.

Table 1. Fundamental data for the streams.

	i/*j*	th_{in}/tc_{in}	th_{out}/tc_{out}	*Fh*/*Fc*	*Lh*/*Lc*	Vh_{in}/Vc_{in}	X_{NH_3}	*p*	Ph_{NH3}/Ph_{NH3}
80%	H1	485.85	351.74	37.90	3736.0	1	0.19523	14,335	2799.68
	H2	309.46	272.8146	38.49	3736.0	0.9537	0.19523	14,140	2760.62
	C1	324.09	450.95	40.07	4302.0	1			555.38
	C2	272.7939	309.45	27.43	3166.0	1			728.84
	C3	283.48	283.5	25.85	1205.0	0			616.10
	C4	268.804	268.930	14.75	704.6	0			361.30
70%	H1	484.05	349.19	32.32	3484.0	1	0.195247	13,450	2624.12
	H2	308.94	272.9670	35.61	3484.0	0.9604	0.195263	13,050	2548.18
	C1	323.31	451.55	33.99	3978.0	1			556.57
	C2	273.1908	308.93	25.60	2964.0	1			713.58
	C3	283.51	283.54	35.05	1607.0	0			616.80
	C4	269.286	269.446	14.81	704.6	0			368.60
60%	H1	481.65	342.98	29.02	3109.0	1	0.192151	11,610	2228.95
	H2	308.98	272.8805	31.12	3109.0	0.9814	0.192144	11,445	2199.16
	C1	319.84	451.55	30.55	3530.0	1			516.46
	C2	272.8280	308.98	22.89	2664.0	1			665.74
	C3	283.95	284.05	44.00	1996.0	0			627.80
	C4	269.429	269.519	9.93	704.6	0			369.90
Utility	HU	473.15	473.15						
	CU	263.15	263.15						

Cost of heat transfer units (€·y^{-1}) = 8333.3·No. Cost of heat transfer area (€·y^{-1}) = 641.7·Area. Price of hot utility = 115.2 €·kW^{-1}·y^{-1}. Price of cold utility = 1.3 €·kW^{-1}·y^{-1}.

The range of values of the uncertain parameters is defined as follows:

- Initial temperatures for H1, H2, C1: ±5 K;
- Initial vapor fraction for H2: 0.01;
- Heat capacity flow rates for C4 (for the remaining streams): ±5 (±10) kW·K^{-1}.

Equations (1) and (2) of substance ammonia are further refined to be used directly in the calculation. The Antoine coefficients A, B, and C take the values of 7.55466, 1002.711, and −25.265, respectively. Note that to make the calculation easier, the units of $Ph^*_{NH3,i,k}$, and $Pc^*_{NH3,j,k}$ are converted from mmHg to kPa by being divided by 0.133.

Equation (3) of substance ammonia is further refined too.$\mathcal{A}$, $\mathcal{B}$, and $\mathcal{C}$ take the values of 4.1856, 60.2724, and 1099.5, respectively.

Equations (6) and (7) are fitted by the process data of ammonia synthesis in this case. For $Rh_{i,k}$, a, b, and c take the values of −0.162, −77.915, and 19,019, respectively; for $Rc_{j,k}$, a, b, and c take the values of −0.322, −55.908 and 22,092, respectively. The fitted curves are shown in Figure 4.

Note that the ratio of hydrogen to nitrogen in the synthesis of ammonia is typically around 3. Therefore, the above formula is an empirical formula based on the experimental data associated with the ratio of hydrogen to nitrogen equal to 3. The saturated ammonia concentration must be raised when a specific amount of noble gas exists, which is why a modified coefficient α is provided. It can also be added to the calculation of gas phase fractions.

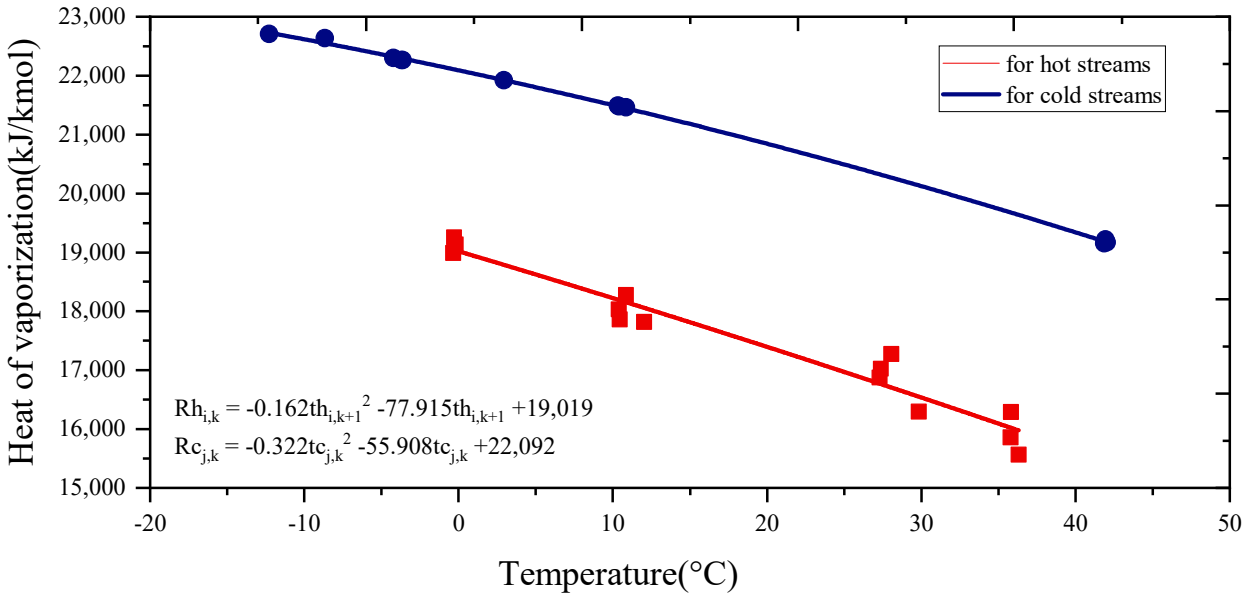

Figure 4. Fitting curves of the heat of vaporization for hot and cold streams.

4.3. Flexible Multiperiod HEN Synthesis

Firstly, due to the natural gas supply shortage, the ammonia synthesis plant operates at about 70% load most of the time. Hence the 70% load operating condition is chosen as the representative subperiod. The data of 70% load in Table 2 are input into Model A, and the representative subperiod HEN topology structure is obtained. It is important to note that due to the process features of ammonia synthesis, such as the sequential distribution of heat exchangers and heat transfer requirements in the combined ammonia cooler, the structure of the HEN has been partially fixed to make the generated HEN more compatible with the actual ammonia synthesis process, such as the combined ammonia coolers part. By determining the nominal structure and solving for the rest of the subperiods, the results for three subperiods and multiperiod are shown in Table 2, where C_c is capital cost, and C_o is operating cost.

Table 2. Optimal structure and area assignment for three subperiods and multiperiod.

Matches (*i*, *j*, *k*)	Heat Transfer Area for Each Load Subperiod/m^2			Nominal Areas/m^2
	60%	70%	80%	
(1, 1, 1)	1520.26	1499.81	1632.53	1632.53
(2, 2, 1)	503.14	590.17	530.13	590.17
(2, 3, 2)	7006.51	7682.36	5607.26	7682.36
(2, 4, 3)	905.29	919.26	928.45	928.45
(HU, 2, 4)	3.39	7.94	11.58	11.58
Total area	9938.59	10,699.54	8709.94	10,845.08
C_c	6.38×10^6	6.91×10^6	5.63×10^6	7.00×10^6
C_o	6606.60	15,323.21	22,392.77	22,392.77
TAC	6.38×10^6	6.92×10^6	5.65×10^6	7.02×10^6

The design of the HEN is shown in Figure 5. The heat exchanger with a shadow indicates phase changes that occur in the corresponding stream during the heat exchange process. Since heat exchanger No. 1 can just meet the heat exchange requirements of H1 and C1 without the involvement of utilities and other heat exchange units, there is no room for flexibility improvement of these two streams. So a cooler CU1 is added at the outlet of H1 and a heater HU1 at the outlet of C1 to adapt a possible flexibility improvement operation. The initial area of two heat exchange units is set to 0 m^2.

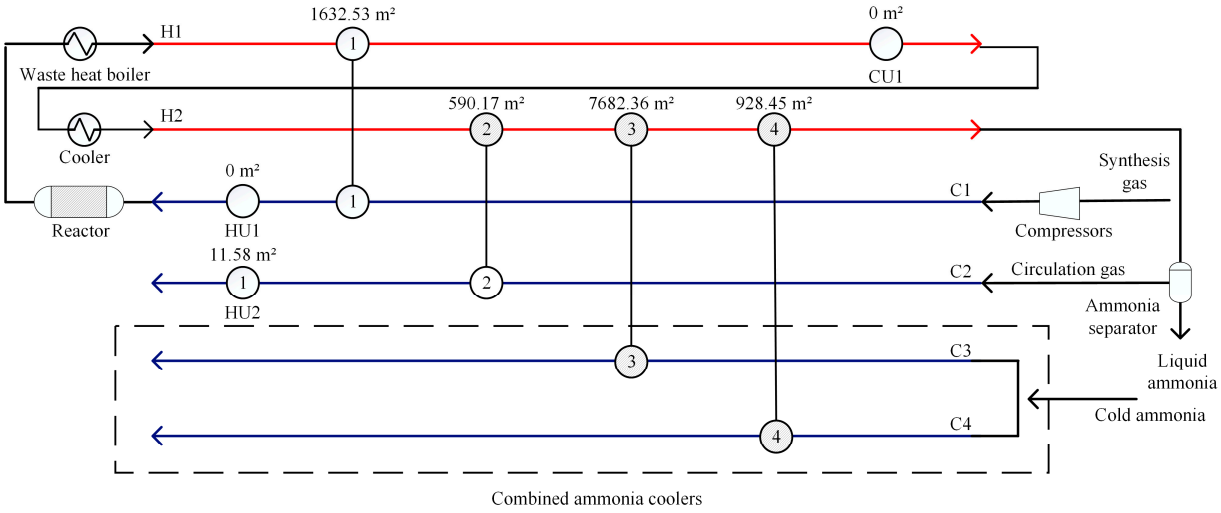

Figure 5. Structure of nominal multiperiod HEN.

After obtaining the results of Model A, the values of the critical points are obtained by solving Model B and are listed in Table 3. Each critical point is a combination of the values of the uncertain parameters t_{in}, t_{out}, V_{in}, and F, where 1 represents that the parameter is at the lower value; 2 represents that the parameter is at the upper value; 3 represents that the parameter is at the inner value; 0 represents that the parameter is not applicable. For example, in the No. 1 critical point, there is an increase in the temperature difference and heat capacity flow rates of the two streams, H1 and C1, associated with the No. 1 heat exchanger, leading to an increase in heat load and a decrease in the approach temperature, resulting in the maximum heat transfer area for the No. 1 heat exchanger.

Table 3. Critical points of the nominal multiperiod HEN.

No.	$th_{in,1}$	$th_{in,2}$	$tc_{in,1}$	$V_{in,2}$	Fh_1	Fh_2	Fc_1	Fc_2	Fc_3	Fc_4
1	2	1	1	1	2	1	2	1	1	1
2	2	0	2	1	2	1	2	2	1	1
3	2	3	2	2	2	2	1	1	1	1
4	2	2	2	2	2	2	1	1	1	1
5	2	1	2	1	2	1	1	1	1	1
6	1	1	1	1	1	1	2	1	1	1
7	2	3	2	1	2	1	1	2	1	1

Then the flexibility indexes of the three subperiods are obtained by Model C calculation. The results show that the values of all three flexibility indexes are 0, which means that the HEN does not pass the flexibility test. In this case, flexible improvement is necessary. By selecting the maximum improved area of the same heat exchanger in different subperiods as the final assigned improved area, the final area of the HEN is determined. The results of Model E are shown in Table 4. Then the flexible indexes need to be rechecked.

Table 4. Area allocation after flexible improvement.

No.	Matches	Nominal	60% Improved	70% Improved	80% Improved	Final Improved	Final Assigned
1	(1, 1, 1)	1632.53					1632.53
2	(2, 2, 1)	590.17					590.17
3	(2, 3, 2)	7682.36					7682.36
4	(2, 4, 3)	928.45	50.22	60.89	63.28	63.28	991.72
5	(1, CU, 4)		161.49	154.30	158.19	161.49	161.49
6	(HU, 1, 0)		408.61	422.39	447.15	447.15	447.15
7	(HU, 2, 0)	11.58	2.04	5.51	8.12	8.12	19.70
	total	10,845.08				680.04	11,525.11

5. Results and Discussion

According to Figure 6, it can be seen that the flexibility indexes of the three subperiods are 1.148, 1.034, and 1, with corresponding area redundancies of 8.36%, 1.34%, and 19.69%, respectively. Since the values of flexibility indexes of three subperiods are greater than 1, it is obvious that this HEN can meet the flexibility requirement.

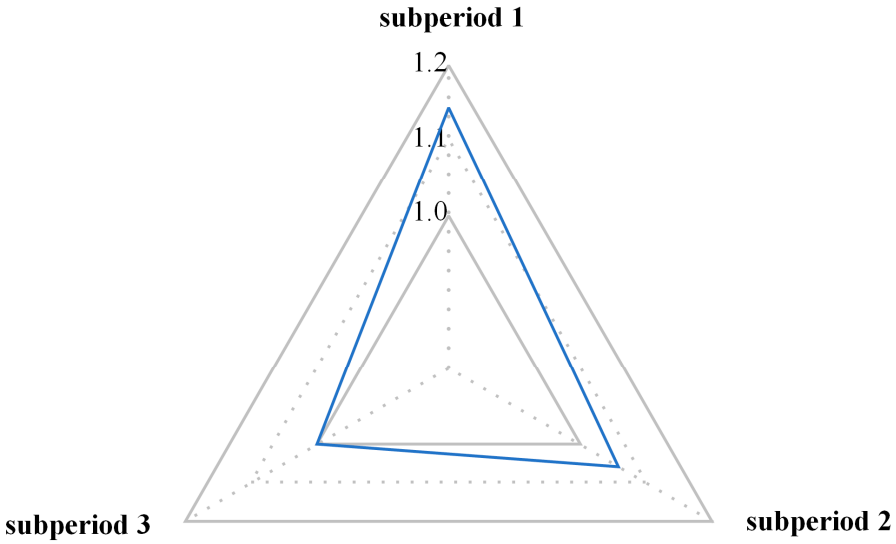

Figure 6. Flexibility indexes of multiperiod HEN in subperiods.

The HEN that has been improved is shown in Figure 7. As can be seen from Figure 7, there is a corresponding increase in area for some of the heat exchange units. This operation aims to give the heat exchanger units the ability to withstand greater heat transfer loads and smaller heat transfer temperature differences.

- The area of heat exchanger No. 4 was increased because the heat transfer load increased, resulting from the increase in the initial temperature and heat capacity flow rates of H2.
- The area of cooler No. 5 and heater No. 6 increased because heat exchanger No. 1, which completely exchanges heat between the hot and cold streams, is unable to meet the heat exchange demand after fluctuations in the initial temperature and heat capacity flow rates of H1 and C1.
- The area of heater No. 7 increased because of a decrease in initial temperature and flow rates of H2 and an increase in heat transfer load with increased heat capacity flow rates of C2.

Comparing Figure 7 with Figure 3, heat exchanger No. 1 corresponds to 121C; heat exchanger No. 2 corresponds to 120C; heat exchanger No. 3 corresponds to 120CF2; heat exchanger No. 4 corresponds to 120CF1; cooler CU1 can be merged with 124C; two heaters, HU1 and HU2, are added to the effective area by calculation of the model, which exists to improve the flexibility of the whole HEN. The heat exchanger with shadow demonstrates that the phase of streams changed during the heat exchange process. When the phase change situation of HEN is checked, we find that H2 of the hot streams and C3 and C4 of the cold streams have different degrees of phase changes. After comparing this result with the actual situation, it is found that the phase change of the streams is consistent. The above results confirm the validity of the phase transition calculation method and the practical feasibility of the whole model.

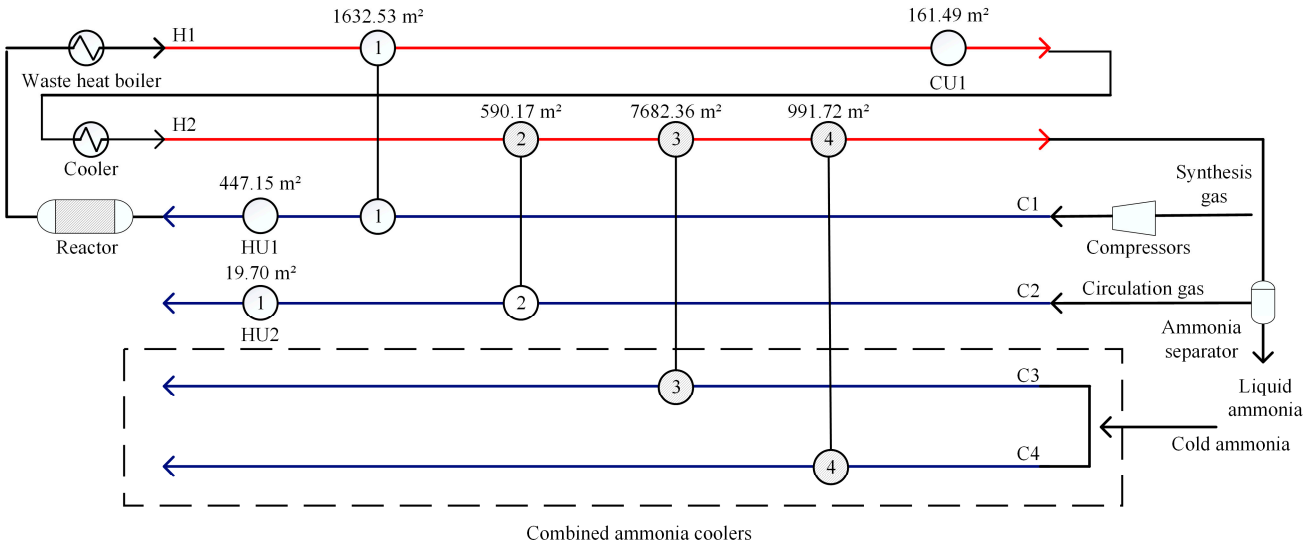

Figure 7. Structure of improved multiperiod flexible HENNo change in area for heat exchangers No. 1, No. 2, and No. 3.

Table 5 shows the comparative results of the four HENs in the number of heat exchangers, heat transfer area, cooling and heating utility loads, capital and operating costs, and total annual costs. The HEN generation model is effective in that the HEN generated reduces the total cost due to the reduced area and the sharing of the heat exchanger load by the hot and cold utilities. It achieved economic optimization and savings for the HEN design of ammonia processes. The heat transfer areas and the respective costs are larger than those calculated by the two models because the actual situation considers more practical elements, such as the sequence of heat exchange. However, the heat transfer area and the flexible HEN's respective costs are inevitably higher than those of the single subperiod because of the subperiod disturbances and the larger range of data fluctuations. This means that not considering the effect of stream data fluctuations when generating a multiperiod HEN leads to failure of the HEN design in practice and results in an underestimation of the cost. Therefore, a better balance between cost and flexibility is essential in HEN design.

Table 5. Comparison of results of four HENs.

Terms	Original	70%	Nominal	Improved
No.	4	5	5	7
Total area	16,841.62	10,699.54	10,845.08	11,525.11
Hot utility	0.00	133.01	193.54	2027.10
Cold utility	0.00	0.00	0.00	1649.74
C_c	1.08×10^7	6.91×10^6	7.00×10^6	7.45×10^6
C_o	0.00	1.53×10^4	2.24×10^4	2.35×10^5
TAC	1.08×10^7	6.92×10^6	7.02×10^6	7.69×10^6

6. Conclusions

In this study, a multiperiod flexible HEN generation method is proposed by considering both the parameter fluctuations of the subperiods and the possibility of the phase changes of the streams. Due to the features of the ammonia process, this method is well-suited to this application. The method first generates a nominal HEN by a representative subperiod approach and a model based on the classical MINLP model, including determining and calculating the phase changes. Then it solves for each heat exchange unit to obtain a critical point as a combination of uncertain parameter values. Finally, the HEN is evaluated for flexibility based on the critical points to confirm its feasibility. If the requirement is not met, a flexibility improvement is carried out, and the improved HEN is tested

again for flexibility. After the method is proposed, it is validated by an actual example of ammonia synthesis. It is concluded that the model can produce an effective multiperiod HEN with phase changes, reduce the total annual cost, and has sufficient flexibility to deal with parameter fluctuations. The method sets the foundation for developing HENs for most industrial multiperiod processes, such as ammonia synthesis with phase changes.

Author Contributions: Conceptualization, S.J. and L.Z.; Data curation, S.J.; Formal analysis, S.J.; Funding acquisition, L.Z.; Investigation, S.J.; Methodology, S.J. and X.J.; Project administration, L.Z.; Resources, S.J., Y.D. and B.D.; Software, S.J. and L.Z.; Supervision, L.Z.; Validation, S.J., L.Z. and X.J.; Visualization, S.J.; Writing—original draft, S.J.; Writing—review and editing, S.J., L.Z., X.J. and Y.D. All authors have read and agreed to the published version of the manuscript.

Funding: This research was funded by the projects (No. 22108178) sponsored by the National Natural Science Foundation of China (NSFC), the National Key Research and Development Program of China (No. 2021YFB4000500), and the special fund for basic scientific research of the central universities (2021CDDZ-01-SCU).

Data Availability Statement: Not applicable.

Conflicts of Interest: The authors declare no conflict of interest.

Nomenclature

Indices	
i	hot stream
j	cold stream
k	superstructure stage
s	critical points
Symbols	
a,b,c	coefficients for the calculation for the heat of vaporization
A,B,C	Antoine coefficients
$\mathcal{A},\mathcal{B},\mathcal{C}$	coefficients for the Larson-Black empirical formula
$Area$	Heat transfer areas, m^2
A	area of the heat exchanger, m^2
Ahu	area of the heater, m^2
Acu	area of the cooler, m^2
$\Delta A_{i,j,k}$	the additional heat transfer areas of heat exchangers, m^2
ΔAhu_j	the additional heat transfer areas of heaters, m^2
ΔAcu_i	the additional heat transfer areas of coolers, m^2
c_a	cost coefficient of heat transfer area, €·m^{-2}·y^{-1}
c_{cu}	cost coefficient of cooling utility, €·kW^{-1}·y^{-1}
c_{hu}	cost coefficient of heating utility, €·kW^{-1}·y^{-1}
c_f	cost coefficient of heat exchanger, €
C_c	Capital cost, €·y^{-1}
C_o	Operating cost, €·y^{-1}
d^A	heat transfer area design variables
d^s	structure design variables
dt	temperature difference for heat exchanger, K
$dthu$	temperature difference for the heater, K
$dtcu$	temperature difference for cooler, K
Fh	heat capacity flow rates for hot streams, kW·K^{-1}
Fc	heat capacity flow rates for cold streams, kW·K^{-1}
g	inequality constraints
g^A	heat transfer area constraints
h	equality constraints
h_v	phase changes constraints
Lh	molar flow rates for hot streams, kmol·h^{-1}

Lc	molar flow rates for cold streams, kmol·h^{-1}
M	a large number
N	No. of subperiods
Nk	No. of stages
No.	No. of units
p	total pressure, kPa
Ph_x	partial pressure of component x for hot streams, kPa
Pc_x	partial pressure of component x for cold streams, kPa
Ph_x^*	saturated vapor pressure of component x for hot streams, kPa
Pc_x^*	saturated vapor pressure of component x for cold streams, kPa
q	heat load, kW
qhu	heating utility, kW
qcu	cooling utility, kW
Rh	the heat of vaporization for hot streams, kJ/kmol
Rc	the heat of vaporization for cold streams, kJ/kmol
sgn	the signum function
TAC	total annual costs, €·y^{-1}
ΔT_{min}	minimum approach temperature, K
th	temperature for hot streams, K
th_{in}	initial temperature for hot streams, K
th_{out}	targeted temperature for hot streams, K
thu_{in}	initial temperature for hot utility, K
thu_{out}	targeted temperature for hot utility, K
tc	temperature for cold streams, K
tc_{in}	initial temperature for cold streams, K
tc_{out}	targeted temperature for cold streams, K
tcu_{in}	initial temperature for cold utility, K
tcu_{out}	targeted temperature for cold utility, K
Vh	vapor fraction for hot streams
Vc	vapor fraction for cold streams
X_x	component content
x	state variables
y	control variables
$y_{NH_3}^*$	equilibrium ammonia content in the vapor
z	1 if the heat exchanger exists, or 0
zhu	1 if the heater exists, or 0
zcu	1 if the cooler exists, or 0
zh	1 if liquefaction exists, or 0
zc	1 if vaporization exists, or 0
Greek letters	
α	a modified coefficient
δ	flexibility index of each subperiod
δ_s	flexibility index of each critical point
θ	uncertain variables
θ^N	nominal uncertain variables
$\Delta\theta$	expected variations of uncertain variables
$\Delta\theta^+$	expected variations of uncertain variables in the positive direction
$\Delta\theta^-$	expected variations of uncertain variables in the negative direction
Ω	the upper bound of heat flow, kW
Γ	the upper bound of temperature difference, K

Appendix A. More Detailed Model A of the Proposed Flexible HEN Synthesis Method

In Model A, there are four sets of constraints: equality constraints, phase change constraints, inequality constraints, and area equality constraints. This model is used to generate a nominal optimal HEN structure of the representative subperiod. Once the topology structure is fixed, the heat transfer area assignment of the HEN for the remaining subperiods is also generated by Model A. The detailed equations are shown below.

Appendix A.1. Equality Constraints

Overall heat balance

$$\begin{aligned} Fh_i(th_{in,i} - th_{out,i}) + zh_{i,k}\sum_k \frac{Lh_i \times Rh_{i,k}\left(Vh_{i,k} - Vh_{i,k+1}\right)}{3600} - \sum_j q_{i,j,k} - qcu_i = 0 \\ Fc_j\left(tc_{in,j} - tc_{out,j}\right) + zc_{j,k}\sum_k \frac{Lc_j \times Rc_{j,k}\left(Vc_{j,k} - Vc_{j,k+1}\right)}{3600} - \sum_i q_{i,j,k} - qhu_j = 0 \end{aligned} \tag{A1}$$

Heat balance at each stage

$$\begin{aligned} Fh_i(th_{i,k} - th_{i,k+1}) + zh_{i,k}\sum_k \frac{Lh_i \times Rh_{i,k} \times \left(Vh_{i,k} - Vh_{i,k+1}\right)}{3600} - \sum_j q_{i,j,k} = 0 \\ Fc_j\left(tc_{j,k} - tc_{j,k+1}\right) + zc_{j,k}\sum_k \frac{Lc_j \times Rc_{j,k} \times \left(Vc_{j,k} - Vc_{j,k+1}\right)}{3600} - \sum_i q_{i,j,k} = 0 \end{aligned} \tag{A2}$$

Hot and cold utility load

$$\begin{aligned} Fh_i(th_{i,nk} - th_{out,i}) - qcu_i = 0 \\ Fc_j\left(tc_{out,j} - tc_{j,1}\right) - qhu_j = 0 \end{aligned} \tag{A3}$$

Assignment of initial temperatures

$$\begin{aligned} th_{in,i} - th_{i,1} = 0 \\ tc_{in,j} - tc_{j,nk} = 0 \end{aligned} \tag{A4}$$

Assignment of vapor fraction

$$\begin{aligned} Vh_{in,i} - Vh_{i,1} = 0 \\ Vc_{in,j} - Vc_{j,nk} = 0 \\ Vh_{out,j} - Vh_{i,nk} = 0 \\ Vc_{i,1} - Vc_{out,j} = 0 \end{aligned} \tag{A5}$$

Assignment of targeted temperatures

$$\begin{aligned} th_{out,j} - th_{i,nk} = 0 \\ tc_{i,1} - tc_{out,j} = 0 \end{aligned} \tag{A6}$$

Appendix A.2. Inequality Constraints

Feasibility of temperatures

$$\begin{aligned} th_{i,k-1} - th_{i,k} \le 0 \\ tc_{j,k+1} - tc_{j,k} \le 0 \\ th_{out,j} - th_{i,nk} \le 0 \\ tc_{i,1} - tc_{out,j} \le 0 \end{aligned} \tag{A7}$$

Feasibility of phase changes

$$\begin{aligned} Vh_{i,k-1} - Vh_{i,k} \le 0 \\ Vc_{j,k+1} - Vc_{j,k} \le 0 \\ Vh_{i,k} - 1 \le 0 \\ Vc_{j,k} - 1 \le 0 \end{aligned} \tag{A8}$$

Constraints of approach temperature

$$\begin{gathered} \Delta T_{min} - \left(th_{i,k} - tc_{j,k}\right) \leq 0 \\ \Delta T_{min} - \left(th_{i,k+1} - tc_{j,k+1}\right) \leq 0 \\ \Delta T_{min} - \left(th_{i,nk} - tcu_{out}\right) \leq 0 \\ \Delta T_{min} - \left(thu_{out} - tc_{j,1}\right) \leq 0 \end{gathered} \tag{A9}$$

Constraints for heat exchanger number

$$\begin{gathered} \sum_{i} z_{i,j,k} \leq 1 \\ \sum_{j} z_{i,j,k} \leq 1 \end{gathered} \tag{A10}$$

Logical constraints for heat exchange

$$\begin{gathered} q_{i,j,k} - \Omega_{i,j} z_{i,j,k} \leq 0 \\ qhu_{j} - \Omega_{j} zhu_{j} \leq 0 \\ qcu_{i} - \Omega_{i} zcu_{i} \leq 0 \end{gathered} \tag{A11}$$

Calculation of approach temperature

$$\begin{gathered} dt_{i,j,k} - \left(th_{i,k} - tc_{j,k}\right) - \Gamma_{i,j}\left(1 - z_{i,j,k}\right) \leq 0 \\ dt_{i,j,k+1} - \left(th_{i,k+1} - tc_{j,k+1}\right) - \Gamma_{i,j}\left(1 - z_{i,j,k}\right) \leq 0 \\ dthu_{j} - \left(th_{i,nk} - tcu_{out}\right) - \Gamma_{j}\left(1 - zhu_{j}\right) \leq 0 \\ dtcu_{i} - \left(thu_{out} - tc_{j,1}\right) - \Gamma_{i}(1 - zcu_{i}) \leq 0 \end{gathered} \tag{A12}$$

Appendix A.3. Equality Area Constraints

$$\begin{gathered} A_{i,j,k} - \left(\tfrac{1}{u} + \tfrac{1}{u}\right) \frac{q_{i,j,k}}{\left(dt_{\,i,j,k} dt_{i,j,k+1}\left(dt_{i,j,k} + dt_{i,j,k+1}\right)/2\right)^{\frac{1}{3}}} = 0 \\ Ahu_{j} - \left(\tfrac{1}{u} + \tfrac{1}{u}\right) \frac{qhu_{j}}{\left(dthu_{\,j}\left(thu_{in} - tc_{out,j}\right)\left(dthu_{j} + thu_{in} - tc_{out,j}\right)/2\right)^{\frac{1}{3}}} = 0 \\ Acu_{i} - \left(\tfrac{1}{u} + \tfrac{1}{u}\right) \frac{qcu_{i}}{\left(dtcu_{\,i}\left(th_{out,i} - tcu_{in}\right)\left(dtcu_{i} + th_{out,i} - tcu_{in}\right)/2\right)^{\frac{1}{3}}} = 0 \end{gathered} \tag{A13}$$

References

1. Floudas, C.A.; Clrlc, A.R.; Grossmann, E. Automatic Synthesis of Optimum Heat Exchanger Network Configurations. *Alche J.* **1986**, *32*, 276–290. [CrossRef]
2. Yee, T.F.; Grossmann, I.E. Simultaneous Optimization Models for Heat Integration—Ii. *Heat Exch. Netw. Synth. Comput. Chem. Eng.* **1990**, *14*, 1165–1184. [CrossRef]
3. Morar, M.; Agachi, P.S. Review: Important Contributions in Development and Improvement of The Heat Integration Techniques. *Comput. Chem. Eng.* **2010**, *34*, 1171–1179. [CrossRef]
4. Yufei, W.; Xiao, F. Progress On Heat Exchanger Network Synthesis and Optimization. *Chem. React. Eng. Technol.* **2014**, *30*, 271–280.
5. Huang, K.F.; Karimi, I.A. Simultaneous Synthesis Approaches for Cost-Effective Heat Exchanger Networks. *Chem. Eng. Sci.* **2013**, *98*, 231–245. [CrossRef]
6. Isafiade, A.; Bogataj, M.; Fraser, D.; Kravanja, Z. Optimal Synthesis of Heat Exchanger Networks for Multi-Period Operations Involving Single and Multiple Utilities. *Chem. Eng. Sci.* **2015**, *127*, 175–188. [CrossRef]
7. Kang, L.; Liu, Y.; Wu, L. Synthesis of Multi-Period Heat Exchanger Networks Based on Features of Sub-Period Durations. *Energy* **2016**, *116*, 1302–1311. [CrossRef]
8. Isafiade, A.J.; Short, M. Simultaneous Synthesis of Flexible Heat Exchanger Networks for Unequal Multi-Period Operations. *Process Saf. Environ. Prot.* **2016**, *103*, 377–390. [CrossRef]
9. Isafiade, A.J.; Short, M.; Bogataj, M.; Kravanja, Z. Integrating Renewables into Multi-Period Heat Exchanger Network Synthesis Considering Economics and Environmental Impact. *Comput. Chem. Eng.* **2017**, *99*, 51–65. [CrossRef]

10. Marselle, D.F.; Morari, M.; Rudd, D.F. Design of Resilient Processing Plants-Ii Design and Control of Energy Management Systems. *Chem. Eng. Sci.* **1982**, *37*, 259–270. [CrossRef]
11. Swaney, R.E.; Grossmann, I.E. An Index For Operational Flexibility in Chemical Process Design. *Alche J.* **1985**, *13*, 621–630. [CrossRef]
12. Konukman, A.E.Ş.; Çamurdan, M.C.; Akman, U. Simultaneous Flexibility Targeting and Synthesis of Minimum-Utility Heat-Exchanger Networks with Superstructure-Based Milp Formulation. *Chem. Eng. Process.* **2002**, *41*, 501–518. [CrossRef]
13. Novak Pintarič, Z.; Kravanja, Z. A Methodology for The Synthesis of Heat Exchanger Networks Having Large Numbers of Uncertain Parameters. *Energy* **2015**, *92*, 373–382. [CrossRef]
14. Pintarič, Z.N.; Kravanja, Z. Identification of Critical Points for The Design and Synthesis of Flexible Processes. *Comput. Chem. Eng.* **2008**, *32*, 1603–1624. [CrossRef]
15. Pintarič, Z.N.; Kasaš, M.; Kravanja, Z. Sensitivity Analyses for Scenario Reduction in Flexible Flow Sheet Design with A Large Number of Uncertain Parameters. *Aiche J.* **2013**, *59*, 2862–2871. [CrossRef]
16. Papalexandri, K.P.; Pistikopoulos, E.N. A Multiperiod Minlp Model for The Synthesis of Flexible Heat and Mass Exchange Networks. *Comput. Chem. Eng.* **1994**, *18*, 1125–1139. [CrossRef]
17. Zhang, W.V.N. Design of Flexible Heat Exchanger Network for Multi-Period Operation. *Chem. Eng. Sci.* **2006**, *61*, 7730–7753. [CrossRef]
18. Aaltola, J. Simultaneous Synthesis of Flexible Heat Exchanger Network. *Appl. Therm. Eng.* **2002**, *22*, 907–918. [CrossRef]
19. Kang, L.; Liu, Y. A Three-Step Method to Improve The Flexibility of Multiperiod Heat Exchanger Networks. *Process Integr. Optim. Sustain.* **2018**, *2*, 169–181. [CrossRef]
20. Ponce-Ortega, J.M.; Jiménez-Gutiérrez, A.; Grossmann, I.E. Optimal Synthesis of Heat Exchanger Networks Involving Isothermal Process Streams. *Comput. Chem. Eng.* **2008**, *32*, 1918–1942. [CrossRef]
21. Luyben, W.L. Heat Exchanger Simulations Involving Phase Changes. *Comput. Chem. Eng.* **2014**, *67*, 133–136. [CrossRef]
22. Yeo, Y.S.; Alwi, S.W.; Ahmad, S.; Manan, Z.A.; Zamzuri, N.H. A New Graphical Method for Heat Exchanger Network Design Involving Phase Changes. *Chem. Eng. Trans.* **2017**, *56*, 1249–1254.
23. Larson, A.T.; Black, C.A. The Concentration Of Ammonia in A Compressed Mixture of Hydrogen And Nitrogen Over Liquid Ammonia. *J. Am. Chem. Soc.* **1925**, *47*, 1015–1020. [CrossRef]
24. Dong, Q.; Jin, Z.; Liu, M. Simulation and Optimization of Heat Exchanger Network for Ammonia Synthesizing Workshop Section. *Mod. Chem. Ind.* **2006**, *Z1*, 304–306.
25. Shaoli, Z.; Jianyang, L.; Jie, Q.; Hui, M.; Tongqing, W.; Guodong, Y. Analysis of Heat Exchanger Networks for Ammonia Systems Based on Pinch Point Technology. *Henan Chem. Ind.* **2018**, *6*, 41–42.